

Charge-changing cross sections for 8–40-MeV $O^{7,8+} + (\text{Ar}, \text{Ne})$ collisions

J. H. Houck, P. A. Závodszy, and J. A. Tanis
 Western Michigan University, Kalamazoo, Michigan 49008
 (Received 17 March 1997)

Absolute cross sections for single- and double-electron capture, and single-electron loss, have been determined for $O^{7,8+}$ ions colliding with Ar and Ne in the energy range 8–40 MeV. Double-electron-capture cross sections were found to be factors of 5–10 smaller than the single-electron capture cross sections. The present results for electron capture from Ar are systematically larger by about 30% than the corresponding cross sections determined previously by Macdonald and Martin [Phys. Rev. A **4**, 1965 (1971)]. The present single-electron-capture cross sections agree well with the empirical scaling rule of Schlachter *et al.* [Phys. Rev. A **27**, 3372 (1983)]. [S1050-2947(97)03909-7]

PACS number(s): 34.50.Fa, 34.70.+e

INTRODUCTION

Charge-changing cross sections in ion-atom collisions are of fundamental and applied interest. For example, such cross sections can be used to test the validity of and to differentiate between various theoretical models. Also, highly accurate charge-changing cross sections are needed for computer simulations of astrophysical and laboratory plasmas.

In this work, total cross section measurements for single-electron capture, double-electron capture, and single-electron loss (from the projectile) were made for 8–40-MeV $O^{7,8+}$ ions impacting on Ar and Ne. The initial motivation for this work arose from other measurements involving zero-degree electron emission in $O^{7,8+} + \text{Ar}$ collisions [1]. More specifically, total cross sections for charge changing were needed to determine the absolute cross sections for electron emission in this related work. The $O^{7,8+} + \text{Ne}$ measurements were conducted because they provide new data and required no change in apparatus or analysis. Single- and double-electron-capture cross sections for $O^{8+} + \text{He}$ were also measured as a benchmark to check the procedures.

EXPERIMENTAL PROCEDURE

This work was done using the Western Michigan University tandem Van de Graaff accelerator. Negative oxygen ions extracted from a duoplasmatron ion source were accelerated, stripped in a gas stripper, and then accelerated again to the final energy. Ions with the desired energy and charge state were selected with an analyzing magnet. These ions were then further stripped with a poststripping foil and the final charge state was selected by a second analyzing magnet. The resulting ion beam was collimated by two apertures, about 2 mm×2 mm and separated by 0.5 m, before entering the target region.

The target region was a differentially pumped gas cell with a geometrical length of about 3.65 cm. The entrance and exit apertures of the cell had diameters of about 3 mm. The target gas pressure was measured with a capacitance manometer, and a feedback voltage to a solenoid valve con-

troller regulated the target cell gas pressure at the desired value.

After passing through the target cell, the ion beam was charge state selected with a third analyzing magnet. The charge-changed components were detected with surface-barrier detectors. The main beam component was collected in a Faraday cup using a suppressor biased to -300 V to prevent electrons from escaping. The current on the Faraday cup was measured with a Keithley electrometer. A 0–2-V output of the electrometer, which is proportional to the Faraday cup current, was dropped across a 1-M Ω resistor. The resulting current was digitized by a current integrator and connected to a scaler to give the incident beam flux. The overall accuracy of the beam current integration (i.e., the accuracy of the electrometer and the digital current integra-

TABLE I. Measured charge-changing cross sections for $O^{7,8+}$ on Ar: σ_{q-2} , double-electron capture; σ_{q-1} , single-electron capture; σ_{q+1} , single-electron loss. The absolute uncertainty in these cross sections is less than $\pm 4\%$.

Projectile	Energy (MeV)	σ_{q-2}	σ_{q-1}	σ_{q+1}
		(10^{-18} cm^2)		
O^{7+}	8	10.8	98.1	0.143
	12	7.35	50.4	0.195
	16	4.79	36.7	0.419
	20	2.80	27.0	0.821
	24	1.57	19.7	1.39
	32	0.520	10.5	2.62
	40	0.174	5.74	3.49
O^{8+}	8	24.4	122	
	10	17.8	77.9	
	12	15.4	59.5	
	14	12.9	49.6	
	16	11.1	43.8	
	20	8.27	34.0	
	24	5.75	26.5	
	32	2.74	16.4	
40	1.36	10.7		

TABLE II. Measured charge-changing cross sections for $O^{7,8+}$ on Ne: σ_{q-2} , double-electron capture; σ_{q-1} , single-electron capture; σ_{q+1} , single-electron loss. The absolute uncertainty in these cross sections is less than $\pm 4\%$.

Projectile	Energy (MeV)	σ_{q-2}	σ_{q-1}	σ_{q+1}
		(10^{-18} cm^2)		
O^{7+}	8	11.9	169	0.0578
	12	4.18	65.4	0.207
	16	1.94	30.3	0.494
	20	0.944	16.2	0.861
	24	0.378	7.84	0.945
	28	0.255	6.58	1.51
	32	0.148	4.65	1.77
	40	0.0619	2.67	2.11
O^{8+}	8	30.4	201	
	10	16.2	127	
	12	10.4	83.1	
	14	7.53	56.4	
	16	5.86	39.4	
	20	3.99	22.3	
	24	2.79	14.2	
	28	1.97	10.2	
32	1.40	7.89		
40	0.706	5.15		

tor) was checked using a calibrated standardized current source.

ANALYSIS

The scattered beam fraction is defined as the ratio of a charged-changed beam component ($q \pm i$) to the total incident beam (q). This scattered beam fraction was measured for several target cell pressure values, from zero to beyond the single-collision regime, for each incident beam energy. As a function of pressure, the scattered beam fraction varies as

$$F_i = a_0 + a_1 P + a_2 P^2 + \dots,$$

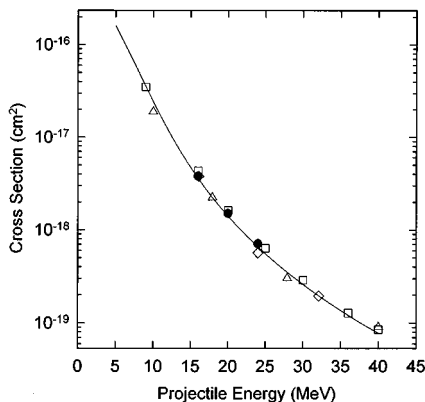


FIG. 1. Benchmark single-capture cross sections for $O^{8+} + He$. Data are as follows: (\bullet), present data; (Δ), Ref. [3]; (\square), Ref. [5]; (\diamond), Ref. [6]. The solid line is the empirical scaling curve of Ref. [2].

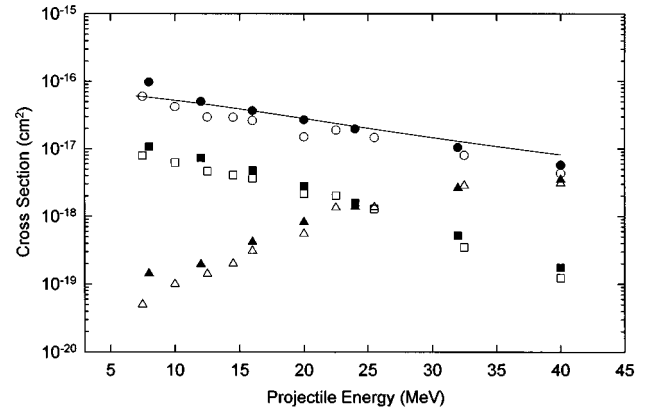


FIG. 2. Charge-changing cross sections for $O^{7+} + Ar$. Data are as follows: single capture: (\bullet), present; (\circ), Ref. [3]; double capture: (\blacksquare), present; (\square), Ref. [3]; electron loss: (\blacktriangle), present; (\triangle), Ref. [3]. The solid curve is the empirical scaling rule of Ref. [4].

where a_0 , a_1 , and a_2 are constants to be determined. For sufficiently low values of the target cell gas pressure, truncation after the quadratic term gives an excellent approximation to the charge-changed fraction. The coefficient a_1 is proportional to the cross section, a_0 is due to the residual gas pressure, and a_2 is the double-collision contribution. Least-squares fits were performed to each F_i versus P plot to determine these coefficients.

The total charge-changed cross section was then determined from

$$\sigma = (kT/L)a_1,$$

where $k = 1.381 \times 10^{-23}$ J/mol K, $T = 295 \pm 3$ K (temperature of the target gas), and $L = 4.1 \pm 0.1$ cm (effective length of the target cell). This gives a total cross section in units of cm^2 of

$$\sigma = (7.49 \times 10^{-15} \text{ cm}^2 \text{ mTorr}) a_1.$$

The target gas temperature T was assumed to be equal to room temperature, which was fairly constant throughout the measurements. The effective length L of the target cell is the geometrical length (3.65 cm) plus a relatively small correction of $(A_1 + A_2)/\sqrt{2}$, where A_1 and A_2 are the entrance and

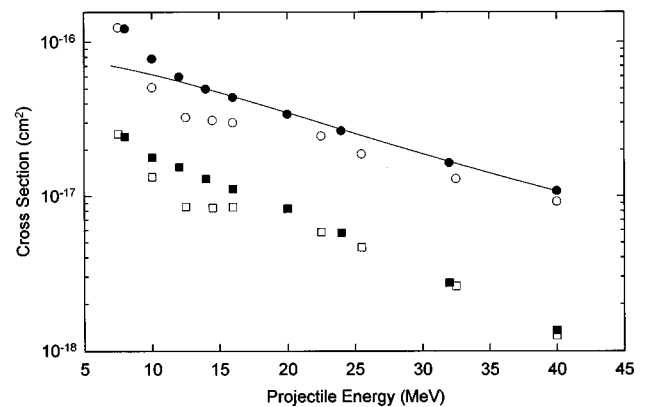


FIG. 3. Charge-changing cross sections for $O^{8+} + Ar$. For key to symbols and curve see caption for Fig. 2.

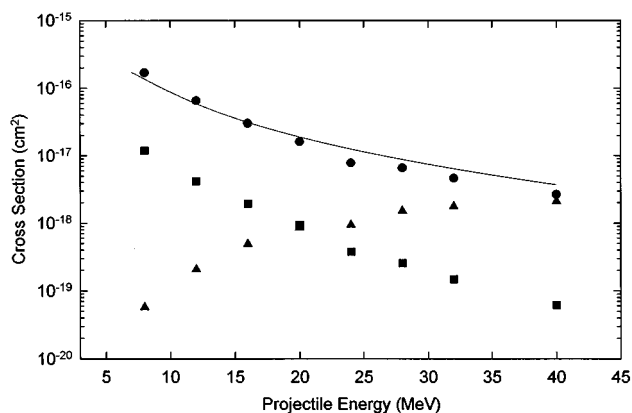


FIG. 4. Charge-changing cross sections for $O^{7+} + Ne$. For key to symbols and curve see caption for Fig. 2.

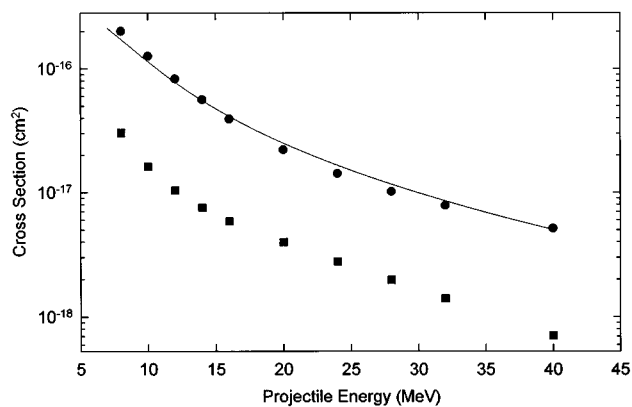


FIG. 5. Charge-changing cross sections for $O^{8+} + Ne$. For key to symbols and curve see caption for Fig. 2.

exit aperture diameters. This correction is due to the fact that the target cell was differentially pumped.

Other systematic errors include the accuracy of the current measurement using the Keithley electrometer ($<1\%$), and the accuracy of the pressure measurement using a capacitance manometer ($<2\%$). The statistical uncertainties in the coefficients a_1 obtained from the least-squares fits were typically less than 1%. Combining all these sources of error in quadrature gives an uncertainty in the measured cross sections of approximately 4%.

RESULTS

Single-capture cross sections for $O^{8+} + He$ were measured as a benchmark and are shown in Fig. 1. It is seen that these data agree well with both previous data of other investigations and with the empirical scaling rule of Schlachter *et al.* [2]. This comparison gives us confidence in the accuracy of our absolute cross-section values.

The present cross-section measurements for single-electron capture, double-electron capture, and single-electron loss for $O^{7,8+} + Ar$ collisions are listed in Table I and are shown in Figs. 2 and 3, along with the previous measurements of Macdonald and Martin [3]. The single- and double-electron-capture cross sections decrease monotonically with increasing beam energy, as expected, with the double-capture cross sections being typically factors of 5–10 smaller than the single-capture cross sections. For $O^{7+} + Ar$ the single-electron loss cross sections increase monotonically with increasing beam energy, reaching values nearly equal to the single-capture cross sections at the highest energies investigated. For both O^{7+} and O^{8+} incident projectiles, the present single-capture cross sections agree well (except the lowest energies for O^{8+}) with the empirical scaling rule of Schlachter *et al.* [4], as they do for $O^{8+} + He$ (Fig. 1).

Noteworthy in the data of Figs. 2 and 3, however, is the fact that the present single- and double-electron-capture cross sections for $O^{7,8+} + Ar$ are systematically larger by about 30% than the corresponding cross sections previously determined by Macdonald and Martin [3]. This discrepancy between the two sets of data is considerably outside the ex-

perimental uncertainty of the present measurements. We believe the present data and uncertainty estimates to be accurate, and hence, the present data serve to provide more precise cross-sectional data for these collision systems. Such results can be important where these charge-changing cross sections are needed for normalization in other related measurements, or in comparisons with theoretical calculations or simulations.

In Table II and in Figs. 4 and 5 are shown the present cross-section measurements for O^{7+} and O^{8+} ions, respectively, colliding with Ne. There are no known earlier measurements for these collision systems. These data exhibit the same qualitative behavior as the data for $O^{7,8+} + Ar$, and they are of nearly the same magnitude. This latter result is a little bit surprising in view of the fact that Ar has more electrons than Ne that can participate in the collision reaction. These additional electrons appear to have little effect on the magnitudes of the cross sections, however. Also, the measured single-electron-capture cross sections are again in good agreement with the empirical scaling rule of Schlachter *et al.* [4], thus providing further evidence for the general applicability and wide range of validity of this scaling rule.

In summary, single-electron capture, double-electron capture, and single-electron loss cross sections are reported for $O^{7,8+} + Ar$ and Ne collisions. The qualitative features of the data follow expected trends for the energy range investigated. The single-capture cross sections are, in all cases, in very good agreement with the empirical scaling rule of Schlachter *et al.* [4]. Of particular note is the fact that the present single- and double-electron-capture cross sections for $O^{7,8+} + Ar$ are about 30% larger than those previously reported by Macdonald and Martin [3]. The accuracy of the present measurements serves to provide more reliable archival data for these latter cross-section values.

ACKNOWLEDGMENT

This work was supported in part by the Division of Chemical Sciences, Office of Basic Energy Sciences, Office of Energy Research, U. S. Department of Energy.

- [1] M. Zhu, R. R. Haar, S. M. Ferguson, O. Voitke, J. A. Tanis, L. Sarkadi, J. Pálinkás, P. A. Závodszky, and D. Berényi, *Nucl. Instrum. Methods Phys. Res. B* **98**, 351 (1995); P. A. Závodszky, E. Y. Kamber, O. Voitke, J. A. Tanis, L. Sarkadi, L. Víkor, J. Pálinkás, D. Berényi, M. Kuzel, and J. McDonald, in *Nineteenth International Conference on the Physics of Electronic and Atomic Collisions, Whistler, British Columbia, Canada, 1995*, Scientific Program and Abstracts of Contributed Papers, edited by J. B. A. Mitchell, J. W. McConkey, and C. E. Brion (Univ. Western Ontario, London, 1995), p. 311.
- [2] A. S. Schlachter, J. W. Stearns, K. H. Berkner, M. P. Stockli, W. G. Graham, E. M. Bernstein, M. W. Clark, and J. A. Tanis, in *Proceedings of the Fifteenth International Conference on the Physics of Electronic and Atomic Collisions, Brighton, United Kingdom, 1987*, edited by J. Geddes, H. B. Gilbody, A. E. Livingston, C. J. Latimer, and H. J. R. Walters (Queen's University, Belfast, 1987), p. 505.
- [3] J. R. Macdonald and F. W. Martin, *Phys. Rev. A* **4**, 1965 (1971).
- [4] A. S. Schlachter, J. W. Stearns, W. G. Graham, K. H. Berkner, R. V. Pyle, and J. A. Tanis, *Phys. Rev. A* **27**, 3372 (1983).
- [5] T. R. Dillingham, J. R. Macdonald, and P. Richard, *Phys. Rev. A* **24**, 1237 (1981).
- [6] R. Hippler, S. Datz, P. D. Miller, P. L. Pepmiller, and P. F. Dittner, *Phys. Rev. A* **35**, 585 (1987).